On the statistical estimation of asymmetrical relationship between two climate variables

Claude Frankignoul, Young-Oh Kwon

Geophysical Research Letters

RESEARCH LETTER
10.1029/2022GL100777

Key Points:

- Composite analysis is biased and always underestimates climate variable asymmetry
- Asymmetric linear regression provides unbiased estimates if the mean of positive and negative events are removed (non-zero intercepts)

Correspondence to:

C. Frankignoul,
claude.frankignoul@locean.ipsl.fr

Citation:

Frankignoul, C., & Kwon, Y.-O. (2022). On the statistical estimation of asymmetrical relationship between two climate variables. *Geophysical Research Letters*, *49*, e2022GL100777. https://doi.org/10.1029/2022GL100777

Received 16 AUG 2022
Accepted 3 OCT 2022

Author Contributions:

Conceptualization: Claude Frankignoul, Young-Oh Kwon
Funding acquisition: Claude Frankignoul, Young-Oh Kwon
Methodology: Claude Frankignoul, Young-Oh Kwon
Project Administration: Young-Oh Kwon
Software: Young-Oh Kwon
Writing – original draft: Claude Frankignoul, Young-Oh Kwon

On the Statistical Estimation of Asymmetrical Relationship Between Two Climate Variables

Claude Frankignoul[1,2] and Young-Oh Kwon[2]

[1]Sorbonne Université, CNRS/IRD/MNHN, UMR LOCEAN, Paris, France, [2]Woods Hole Oceanographic Institution, Woods Hole, MA, USA

Abstract Two simple methods commonly used to detect asymmetry in climate research, composite analysis, and asymmetric linear regression, are discussed and compared using mathematical derivation and synthetic data. Asymmetric regression is shown to provide unbiased estimates only when the respective mean of positive and negative events is removed from both independent and dependent variables (i.e., non-zero *y*-intercepts). Composite analysis always provides biased results and strongly underestimates the asymmetry, albeit less so for very larger thresholds, which cannot be used with limited observational data. Hence, the unbiased asymmetric regression should be used, even though uncertainties can be large for small samples. Differences in estimated asymmetry are illustrated for the sea surface temperature and winter sea level pressure signals associated with El Niño and La Niña.

Plain Language Summary There is increasing evidence of asymmetry in climate variability so that the response to a positive event may not always be opposite to that of a negative event. The most common method to estimate such asymmetry is by compositing sufficiently large positive and negative events. We demonstrate that composites are always biased and underestimate asymmetry, albeit less so for large threshold. Unbiased estimates can be obtained by separate regressions on positive and negative events provided their respective mean is removed. This is illustrated with synthetic data and an application to El Niño and La Niña sea surface temperature signals and winter sea level pressure teleconnections to extratropical latitudes.

1. Introduction

The strong asymmetry of sea surface temperature (SST) and climate variability in the tropics has long been known, as illustrated by the marked differences between the positive (El Niño) and negative phase (La Niña) of the El Niño-Southern Oscillation (e.g., Okumura & Deser, 2010; Timmermann et al., 2018). The asymmetry of the ENSO teleconnections to extratropical latitudes is more debated, as some studies report symmetric signals (e.g., Deser et al., 2017) while others find asymmetry (e.g., Hardiman et al., 2019), often based observationally on composites that compare the sea level pressure (SLP) or other atmospheric variable associated with large positive and negative values of an index of the ENSO SST variability. There is also growing observational (Frankignoul et al., 2011; Révelard et al., 2016; Seo et al., 2017) and modeling evidences (Seo et al., 2017) that the atmospheric response to western boundary currents meridional shifts may be asymmetric, hence that the atmospheric response to a northward shift of the current is not opposite to that to a similar southward shift. Using composite analysis, Révelard et al. (2016) found that the atmospheric response to dynamical states of the Kuroshio Extension is significant for its stable (northward) state while no evidence of a significant signal was found for the unstable (southward) state. Such result suggests that methods only searching for symmetric responses, such as standard linear regression, may underestimate or overestimate a response, if the actual responses are asymmetric. In fact, if asymmetry is so strong that similar responses of the same sign occurred in opposite states, as in some numerical simulations of the remote atmospheric response to wintertime SST variability in the East/Japan Sea (Seo et al., 2014), standard linear regression analysis of observations would fail to detect any response, and so would symmetric analysis (i.e., response to positive minus response to negative phases) in atmospheric response studies (as in Smirnov et al., 2015). In circumstances that may involve nonlinear dynamics and eddy-mean flow interactions, it is thus important to verify the symmetry of a detected atmospheric response, hence to establish how asymmetric responses can be best assessed.

In the present paper, we discuss two methods commonly used to detect asymmetry in the atmospheric response to SST anomalies, namely composite analysis or compositing (e.g., Deser et al., 2017; Mezzina et al., 2002)

and asymmetric linear regression (e.g., Frankignoul et al., 2011), as they can easily be applied to observational products and do not require the large samples that are often needed in statistical learning, causal effect networks, and other nonlinear methods. We further discuss the two different ways to apply the asymmetric regression, with fixed-zero or non-zero y-intercepts. Using mathematical derivation and a simple synthetic example, we show that the commonly used composite analysis may strongly underestimate the response asymmetry, while unbiased estimates can be obtained by asymmetric regression with non-zero y-intercepts, as least if linearity holds for the response to SST anomalies of the same sign.

2. An Asymmetric Example

To easily compare how asymmetry is estimated from observations, we introduce a model that mimics in a very simple way the asymmetry of the atmospheric response to oceanic anomalies. Let N observations of an oceanic anomaly (e.g., an El Niño SST index) be represented by the time series $x(j)$ for $j = 1, N$. The sample mean of the oceanic anomalies, $\overline{x(j)} = \frac{1}{N}\left(\sum_1^{N_p} x_p + \sum_1^{N_n} x_n\right)$, is by definition of an anomaly equal to zero. Here x_p is positive and x_n negative, and there are N_p positive and N_n negative x-values, $N = N_p + N_n$.

To represent an asymmetric atmospheric response, we assume that an atmospheric variable y is given by a term proportional to the oceanic anomalies plus an uncorrelated noise ε with zero mean that represents intrinsic atmospheric variability and has the same variance in positive and negative cases,

$$y_p(k) = \alpha x_p(k) + \varepsilon(k) \tag{1}$$

$$y_n(r) = x_n(r) + \varepsilon(r), \tag{2}$$

where k corresponds to positive x's and r to negative x's. The true response to negative x-values is taken for simplicity to be x_n while that to positive x-values is given by $\alpha\, x_p$. The true asymmetry is given by the ratio of the slopes α:1.

The sample mean of y is given b y

$$\overline{y} = \frac{1}{N}\left(\sum_1^{N_p} y_p + \sum_1^{N_n} y_n\right) = \alpha\frac{N_p}{N}\overline{x_p} + \frac{N_n}{N}\overline{x_n} \approx \frac{\alpha - 1}{2}\overline{x_p}, \tag{3}$$

if one assumes for simplicity that there are as many positive N_p and negative N_n events. Then, atmospheric anomalies $Y(k)$, as used in observational analyses, are defined as departures from the sample mean and thus have zero mean. This is obtained by subtracting $\overline{y}$ in Equations 1 and 2,

$$Y_p(k) = y_p(k) - \overline{y} \approx \alpha x_p(k) + \varepsilon(k) - \frac{\alpha - 1}{2}\overline{x_p} \tag{4}$$

$$Y_n(r) = y_n(r) - \overline{y} \approx x_n(r) + \varepsilon(r) - \frac{\alpha - 1}{2}\overline{x_p}, \tag{5}$$

Neglecting the noise means, one has $\overline{Y_p} \approx \frac{\alpha+1}{2}\overline{x_p}$, $\overline{Y_n} \approx -\frac{\alpha+1}{2}\overline{x_p}$, hence $\overline{Y_p}$and$\overline{Y_n}$ are equal and opposite, and $\overline{Y} = \overline{Y_p} + \overline{Y_n} \approx 0$. Observational atmospheric and oceanic anomalies would therefore be represented in this example by the Y and x time series, respectively.

3. Asymmetric Regression

3.1. Zero-Intercept Regression (Method 1)

If one assumes that positive and negative events are represented by two regression models with fixed-zero intercepts

$$Y_p(k) = a_p x_p(k) + e(k) \tag{6}$$

$$Y_n(r) = a_n x_n(r) + e(r) \tag{7}$$

where e is the residual, the a_p estimator of the true slope α is, using Equation 4,

$$a_p \approx \sum_1^{N_p} \left(\alpha\, x_p(k)x_p(k) - \frac{\alpha-1}{2}x_p(k)\overline{x_p}\right)/\sum_1^{N_p} x_p(k)x_p(k) \approx \alpha - N_p\,\frac{\alpha-1}{2}\overline{x_p}^2/\sum_1^{N_p} x_p(k)x_p(k) \quad (8)$$

If $\alpha > 1$, the estimator a_p of the true slope α is negatively biased, while the estimator a_n of the true slope 1 is positively biased as one has from Equation 5

$$a_n \approx \sum_1^{N_n} \left(x_n(r)x_n(r) - \frac{\alpha-1}{2}x_n(r)\overline{x_p}\right)/\sum_1^{N_n} x_n(r)x_n(r) \approx 1 + N_n\,\frac{\alpha-1}{2}\overline{x_p}^2/\sum_1^{N_n} x_n(r)x_n(r) \quad (9)$$

Hence, the true asymmetry α:1 is underestimated. If $\alpha < 1$, it is easy to show that the asymmetry is also underestimated. If x follows a standardized Gaussian distribution, one has $\overline{x_p} = 0.8$, $N^{-1}\sum_1^{N_p} x_p(k)x_p(k) = 0.5$ (half the unit variance). The amplitude of the bias should then be $0.64\frac{\alpha-1}{2}$.

The method 1 is biased because the regression intercepts are assumed to be zero, leading to an inconsistency. Indeed, from Equations 6 and 7, one has $\overline{Y_p} \approx a_p\overline{x_p}$, $\overline{Y_n} \approx a_n\overline{x_n}$ if the means of the residuals are neglected. Hence, since $\overline{x_n} = -\overline{x_p}$, $\overline{Y} \approx \left(a_p - a_n\right)\overline{x_p}$ would require $a_p = a_n$ to satisfy $\overline{Y} = 0$.

3.2. Non-Zero Intercept Regression (Method 2)

For this second approach, we apply the asymmetric regressions with fixed y-non-zero intercepts, that is, after removing the means for positive and negative values of the independent (oceanic) variable, respectively, and correspondingly for the dependent (atmospheric) variable. For positive events, let

$$Y_p(k) - \overline{Y_p} = A_p\left(x_p(k) - \overline{x_p}\right) + e(k) \quad (10)$$

where A_p denote the estimate of the true slope α and e is the residual. Using Equation 4 and $\overline{Y_p} \approx \frac{\alpha+1}{2}\overline{x_p}$, one has

$$\begin{aligned} A_p = \sum_1^{N_p}\left(Y_p(k) - \overline{Y_p}\right)\left(x_p(k) - \overline{x_p}\right)/\sum_1^{N_p}\left(x_p(k) - \overline{x_p}\right)^2 \approx \sum_1^{N_p}\left(\alpha x_p(k) - \alpha\overline{x_p}\right) \\ \left(x_p(k) - \overline{x_p}\right)/\sum_1^{N_p}\left(x_p(k) - \overline{x_p}\right)^2 \approx \alpha \end{aligned} \quad (11)$$

Similarly, for negative events let

$$Y_n(r) - \overline{Y_n} = A_n\left(x_n(r) - \overline{x_n}\right) + e(r) \quad (12)$$

where A_n denotes the estimate of the true slope 1. One has

$$\begin{aligned} A_n = \sum_1^{N_n}\left(Y_n(r) - \overline{Y_n}\right)\left(x_n(r) - \overline{x_n}\right)/\sum_1^{N_n}\left(x_n(r) - \overline{x_n}\right)^2 \approx \sum_1^{N_n}\left(x_n(r) + \overline{x_p}\right) \\ \left(x_n(r) + \overline{x_p}\right)/\sum_1^{N_n}\left(x_n(r) + \overline{x_p}\right)^2 \approx 1 \end{aligned} \quad (13)$$

Therefore, the estimated slopes are unbiased and model 2 should be preferred. Note that the method 2 is quickly asymptotically equivalent in sample size to fitting a regression with slope and intercept parameters to both the positive and negative x values, and that for $x_p = x_n = 0$, one has $Y_p \approx -\frac{\alpha-1}{2}\overline{x_p} + e$, $Y_n \approx -\frac{\alpha-1}{2}\overline{x_p} + e'$. Hence, there is no discontinuity in the linear fit.

4. Composites (Method 3)

Composites are built by selecting positive and negative values of x and comparing the corresponding values of Y, usually based on sample means. The simplest composites would consider all values of the same sign, thus comparing $\overline{Y_p}$ to $\overline{x_p}$ and $\overline{Y_n}$ to $\overline{x_n}$, but there would be no asymmetry since $\frac{\overline{Y_p}}{\overline{x_p}} \approx \frac{\overline{Y_n}}{\overline{x_n}}$. To detect asymmetry, composites must be based on large absolute values of x generally obtained by selecting x-values larger or smaller than a given threshold. How it compares to the true solutions depends on the probability density function (pdf) of x and ε. We consider two simple cases and illustrate them for $a = 3$, a relatively strong asymmetry that is used in the synthetic examples below.

4.1. Uniform x-Distribution

Because it is analytically simple, we first consider the case where x is uniformly distributed in the interval (−50, 50). The pdf $f(x)$ is given by:

$$\begin{aligned} f(x) &= 1/100 \text{for} x \in (-50, 50) \text{and zero otherwise} \\ f\left(x_{\mathrm{p}}\right) &= 1/50 \text{for} x \in (0, 50) \text{and zero otherwise} \\ f\left(x_{\mathrm{n}}\right) &= 1/50 \text{for} x \in (-50, 0) \text{and zero otherwise.} \end{aligned} \tag{15}$$

The expected values are $\overline{x_{\mathrm{p}}} = 25$, $\overline{x_{\mathrm{n}}} = -25$, variance $(x) = 100^2/12$. Based on a sample of $N/2$ positive values and $N/2$ negative values, one would have $\overline{x_{\mathrm{p}}} = 25 \pm 100/(6N)^{\frac{1}{2}}$, $\overline{x_{\mathrm{n}}} = -25 \pm 100/(6N)^{1/2}$, where the error is given by the standard error (SE).

For very large sample, say $N = 10{,}000$, the estimation errors are very small, $\overline{x_{\mathrm{p}}} = 25 \pm 0.41$. Composites based on the 25% largest and smallest values yield $\overline{x_{\mathrm{p25}}} = 37.5 \pm 0.58$, $\overline{x_{\mathrm{n25}}} = -37.5 \pm 0.58$. Neglecting the small averaging errors and using Equations 4 and 5 with $\alpha = 3$, the estimated asymmetry is given by $\left(\frac{\overline{Y_{\mathrm{p25}}}}{\overline{x_{\mathrm{p25}}}}\right) \approx \alpha - \frac{\alpha-1}{2}\frac{25}{37.5} \approx 2.33$, $\left(\frac{\overline{Y_{\mathrm{n25}}}}{\overline{x_{\mathrm{n25}}}}\right) \approx 1 + \frac{\alpha-1}{2}\frac{25}{37.5} \approx 1.67$. Based on 1 SE of the means, the corresponding ranges are, assuming for simplicity uncorrelated errors in $\overline{x_{\mathrm{p25}}}$ and $\overline{x_{\mathrm{p}}}$, given by $\left(\frac{\overline{Y_{\mathrm{p25}}}}{\overline{x_{\mathrm{p25}}}}\right) \approx \frac{112.5 \pm 1.74 - 25 \pm 0.41}{37.5 \pm 0.58} \approx \frac{87.5 \pm 1.74}{37.5 \pm 0.58} \pm \frac{0.41}{37.5} \approx$ (2.31–2.35), and similarly $\left(\frac{\overline{Y_{\mathrm{n25}}}}{\overline{x_{\mathrm{n25}}}}\right) \approx \frac{62.5 \pm 0.58}{37.5 \pm 0.58} \pm \frac{0.41}{37.5} \approx$ (1.65–1.69) if the errors in $\overline{\varepsilon}$ are neglected, and broader otherwise. Therefore, the asymmetry is strongly underestimated. Larger thresholds decrease the biases, but do not cancel it since the top and bottom 1% composites yield $\left(\frac{\overline{Y_{\mathrm{p1}}}}{\overline{x_{\mathrm{p1}}}}\right) \approx \alpha - \frac{\alpha-1}{2}\frac{25}{49.5} \approx 2.49$, $\left(\frac{\overline{Y_{\mathrm{n1}}}}{\overline{x_{\mathrm{n1}}}}\right) \approx 1 + \frac{\alpha-1}{2}\frac{25}{49.5} \approx 1.51$. The biases increase with α, thus with the true asymmetry.

For small sample, say $N = 100$, one has $\overline{x_{\mathrm{p25}}} = 37.5 \pm 5.8$, $\overline{x_{\mathrm{p}}} = 25 \pm 4.1$, $\overline{x_{\mathrm{n25}}} = -37.5 \pm 5.8$. Neglecting errors in $\overline{\varepsilon}$ and the correlation between errors in $\overline{x_{\mathrm{p25}}}$ and $\overline{x_{\mathrm{p}}}$, for $\alpha = 3$ one obtains $\left(\frac{\overline{Y_{\mathrm{p25}}}}{\overline{x_{\mathrm{p25}}}}\right) \approx \frac{112.5 \pm 17.4 - 25 \pm 4.1}{37.5 \pm 5.8} \approx \frac{87.5 \pm 17.4}{37.5 \pm 5.8} \pm \frac{4.1}{37.5}$ and $\left(\frac{\overline{Y_{\mathrm{n25}}}}{\overline{x_{\mathrm{n25}}}}\right) \approx \frac{62.5 \pm 5.8}{37.5 \pm 5.8} \pm \frac{4.1}{37.5}$, which yields larger ranges of about (2.10–2.53) and (1.43–1.94), respectively. Adding uncertainty in $\overline{\varepsilon}$ further broadens these ranges. For instance, if ε has the same but independent uniform distribution as x in Equation 15, as in the synthetic example below, one has $\overline{\varepsilon_{\mathrm{p25}}} \approx \overline{\varepsilon_{\mathrm{n25}}} \approx \pm 5.8$, and the approximate ranges become (2.02–2.61) and (1.35–2.02). For uniform x-distributions, composites are always biased and underestimate the asymmetry.

4.2. Gaussian Distribution

The Gaussian case is more relevant to observations. In the present example, one can get insights from Equations 4 and 5. For very large absolute x-values (e.g., $x_{\mathrm{p}} \gg \overline{x_{\mathrm{p}}}$), one has $Y_{\mathrm{p}}(k) \approx \alpha x_{\mathrm{p}}(k) + \varepsilon(k)$ and $Y_{\mathrm{n}}(r) \approx x_{\mathrm{n}}(r) + \varepsilon(r)$, so that unbiased estimates could be obtained. However, in observations or even climate model simulations, such very large values of x never occur, and for reasonable thresholds the estimated asymmetry degrades rapidly. For example, for positive and negative x-values twice their mean and $\alpha = 3$, $Y_{\mathrm{p}}(k) = 5\ \overline{x_{\mathrm{p}}} + \varepsilon(k)$, and $Y_{\mathrm{n}}(r) = 3\ \overline{x_{\mathrm{n}}} + \varepsilon(r)$, hence the expected asymmetry is substantially biased (i.e., 5:3 instead of 3:1 for the true values). The expected biases could be derived from the pdf of x and e by integrating over all x above or below an assumed threshold, but instead we simply use synthetic data in Section 5 to show that the composites are biased even with large thresholds.

5. Numerical Solutions

5.1. Uniform x-Distribution

Synthetic data with zero mean and $N = 100$ are randomly generated from Equations 1 and 2 for uniform predictor x and noise ε distribution in (−50, 50) with $\alpha = 3$. A realization of the x and $Y = y - \overline{y}$ data for is shown in Figure 1a, where x should be viewed as the oceanic anomaly and y as the atmospheric response to x. In Figure 1a, three different estimates of the asymmetry are represented and the results of 1,000 random simulations are in Figure 1b. For $N = 100$, the regression method 1 (Section 3.1) is biased and underestimates the slope for positive

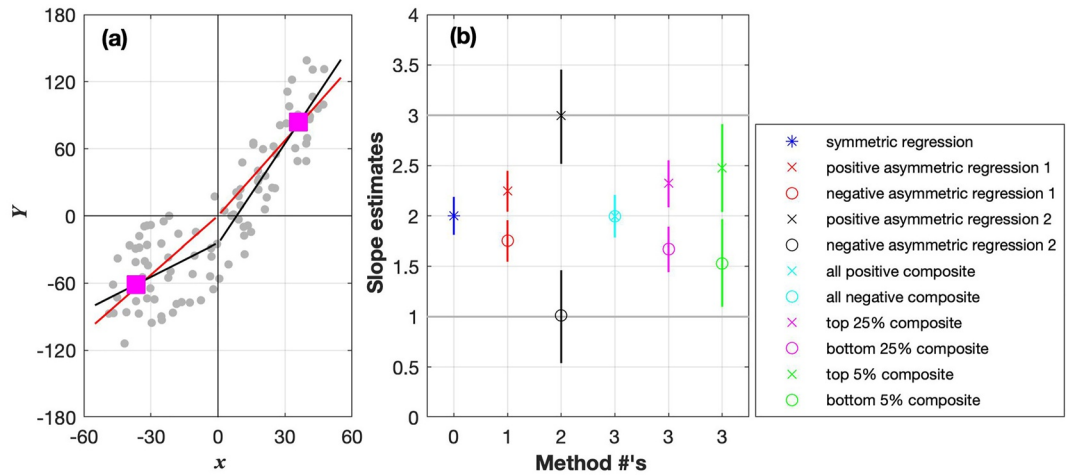

Figure 1. (a) Scatter plot of a realization of the synthetic x and Y series with uniform x and ε distribution in $(-50, 50)$ and $\alpha = 3$ with $N = 100$. The symmetric regression by method 0 and the asymmetric regressions by methods 1 and 2 are represented, as well as composite based on a 25% threshold (method 3). (b) Results of 1,000 random simulations. The colored symbols indicate the mean values of the estimated slopes and the composite threshold, and the vertical bars indicate 95% interval from the 1,000 iterations. Crosses correspond to positive x-values and circles to negative ones, and the horizontal lines indicate the true slopes.

events and overestimates the slope for negative ones by 0.75, as is predicted by Equations 8 and 9, thus strongly underestimating asymmetry (i.e., 2.25:1.75 instead of 3:1). Note that the standard (symmetric) regression (blue star, method 0) based on all x-values provides even more biased estimates of the true slopes since it does not distinguish between positive and negative x-values. On the other hand, the slope estimates are unbiased with the method 2 (Section 3.2), as expected. However, the error bar with the method 2 is rather large, more than twice that with the method 1. Note that the error bars are highly similar for positive and negative x-values since they only depend on N and ε.

Composite analysis (method 3) is also biased. As discussed in Section 4.1, composite based on all positive or negative values are unable to detect asymmetry. Consistent with our analysis, the biases in the slopes are larger for the 25% composites than for the 5% composites that indeed get close to the limit obtained for infinite sample (2.5:1.5), albeit with large uncertainty (nearly as large as with the regression method 2) since the sample is more limited. Interestingly, the 25% composites and the regression method 1 yield comparable estimates, but it occurs because they turned out to be similarly biased.

5.2. Gaussian Distribution

A second set of synthetic data was generated for $\alpha = 3$ using standardized Gaussian distribution for the predictor variable x and the noise ε, so that expected values are $\overline{x_p} = 0.8, \overline{x_n} = -0.8, \frac{\sum_1^{N_p} x_p(k) x_p(k)}{N} = 0.5$ (half the unit variance). Figure 2 compares the different estimates of the slope for (left) $N = 100$ and (right) $N = 10{,}000$ random x and ε samples. As above, the synthetic data are randomly generated 1,000 times to document the uncertainty of each estimate. The mean values of the asymmetric regressions do not significantly depend on N, but the uncertainties are of course much larger for $N = 100$ (they coarsely scale as $N^{-1/2}$). In fact, the 95% confidence intervals are essentially negligible for $N = 10{,}000$.

From Equations 8 and 9 the mean biases of the asymmetric regression method 1 are large (≈ 0.64), consistent with Figure 2. For $N = 100$, the 95% confidence intervals are small, so there is negligible chance to obtain the true values. As predicted, the method 2 is unbiased, and the 95% confidence interval, albeit larger, is somewhat smaller than for uniform distributions. In our example for $N = 100$, the ranges of estimated slopes in 1,000 simulations were (2.35–3.75) for positive x and (0.25–1.8) for negative x. Hence, relative estimation errors can be large, in particular if the true slope is small as was the case for negative x.

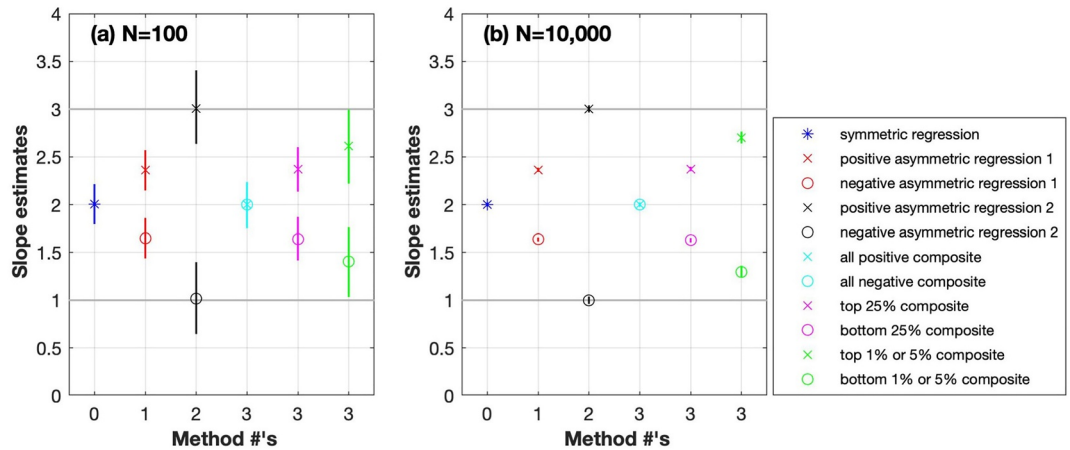

Figure 2. As in Figure 1, but using synthetic data generated using x and e from standardized Gaussian distribution and $\alpha = 3$ with (a) $N = 100$ and (b) $N = 10{,}000$. Note that (a) uses 5% threshold for the most extreme composites, while (b) uses 1%. Crosses correspond to positive x-values and circles to negative ones.

Composite based on a 25% threshold are also strongly biased, and again comparable to those of the regression method 1, albeit with slightly larger uncertainties. For $N = 100$, the 95% confidence interval is (2.1–2.6) for positive x and (1.4–1.9) for negative x, while the full ranges were (1.9–2.9) and (1.1–2.1), respectively, so they did not even overlap with the true values. Composites based on the 5% largest or smallest x-values provide better, but still biased estimates of the asymmetry, and the 95% confidence intervals remain far from the true values. However, estimates could occasionally match or even exceed the true slope since the full ranges in 1,000 simulations were (2.0–3.3) for positive x and (0.6–2.0) for negative x. For $N = 10{,}000$, an unreasonable case for observed climate time series, composites based on a more extreme 1% threshold could be considered, but they remain biased, nearly as much as for the 5% threshold (not shown). Composite analysis thus always underestimates the asymmetry, as shown in Section 4.

6. Application to ENSO

To illustrate the differences between the three methods using observations, we consider the SST signature of El Niño and La Niña events and their teleconnections in boreal winter (DJF), even though ENSO time series have some skewness. We use the HadISST (Rayner et al., 2003) for SST and the NCEP-NCAR R1 (Kistler et al., 2001) for SLP in the period 1948–2018. After removing the mean seasonal cycle and a cubic trend from the monthly values, time series of the DJF mean Niño3.4 index as well as SST and SLP anomalies are constructed. Regressions are on the DJF Niño3.4 index. Composites are based on 10% percentile, a larger threshold than most analyses, which are based on values larger or smaller than 1 standard deviation of the Niño3.4 index (e.g., Deser et al., 2017; Mezzina et al., 2022). Our choice results in seven El Niño and seven La Niña events. Note that the units in Figure 3 are per positive or negative index (i.e., °C/°C), so that the sign of the negative case should be inverted to display La Niña signals.

The asymmetry in the SST anomalies between positive and negative cases is most noticeable in the location of the maximum anomalies, which is found in the central equatorial Pacific in the negative (La Niña) case but shifted eastward in the positive (El Niño) case. However, the local amplitudes exhibit the asymmetry consistent with our mathematical derivation and synthetic examples, as the amplitudes in the eastern Pacific is larger for the positive phase and the asymmetry is largest for regression method 2 and smallest for regression method 1. For example, at 90°W on Equator, the regression method 2 gives 1.30°C/°C and 0.38°C/°C for the positive and negative phases, respectively, while the regression method 1 and the composite give 0.93°C/°C versus 0.60°C/°C and 1.05°C/°C versus 0.49°C/°C, respectively. On the other hand, the SST amplitude in the central Pacific is slightly larger for the negative phase, but the asymmetry is again largest for regression method 2. For example, the amplitudes at 165°W on Equator for the positive versus negative phases are 1.17°C/°C versus 1.25°C/°C, 1.06°C/°C versus 1.29°C/°C, and 1.14°C/°C versus 1.27°C/°C for regression model 1, regression model 2, and composite, respec-

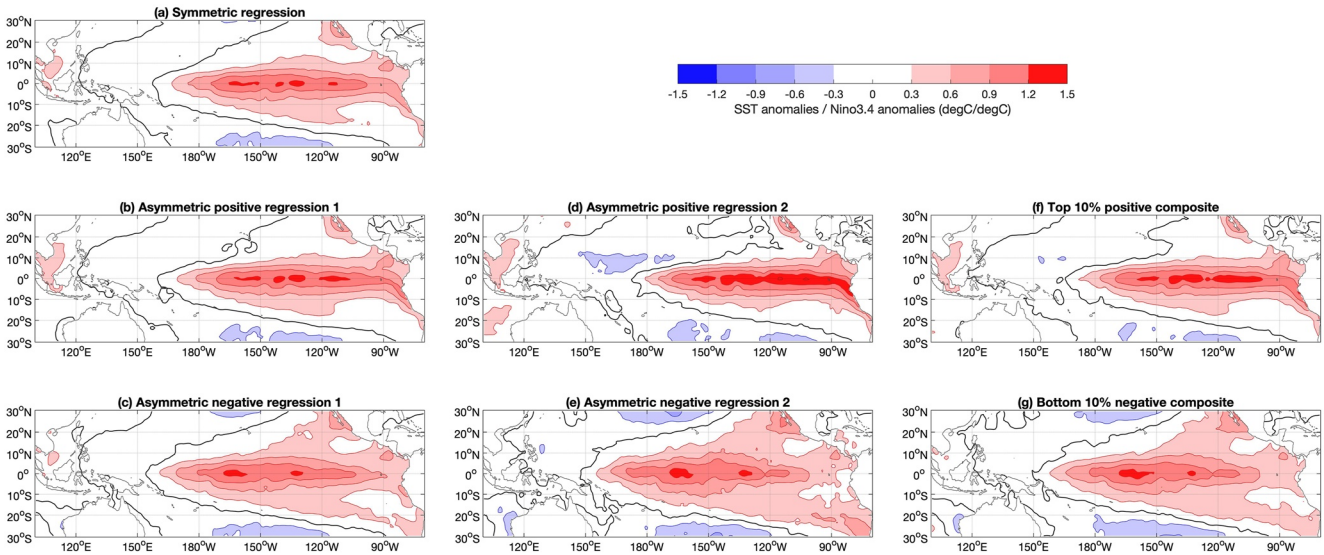

Figure 3. Sea surface temperature (in °C/°C with contour interval of 0.3°C/°C) associated with positive and negative values of the Niño3.4 index in DJF. Estimates were made by (a) standard regression, (b and c) asymmetric regression 1, (d and e) asymmetric regression 2, and (f and g) composites based on a 10% threshold (seven El Niño and seven La Niña events).

tively. Therefore, the asymmetry is largest for regression model 2, and smallest for regression model 1 with the composites in between.

The SLP regressions are more contrasted in amplitude and pattern, showing a strong Aleutian Low for El Niño and a much weaker, southwestward shifted low for La Niña (Figure 4). Consistent with our analysis, the strongest Aleutian Low deepening is given by regression method 2 and the weakest by regression method 1. The composites are based on a high threshold and are thus in-between, consistent with our mathematical derivation and synthetic examples (Figure 2).

7. Summary and Discussion

We have shown that asymmetry is best estimated by asymmetric regression models with fixed non-zero *y*-intercepts (method 2), which provide unbiased slope estimates. However, for limited samples as often found in observational analyses, errors in the estimated slopes can be large, in particular if the true slopes are small and the noise is larger than considered here. Asymmetric regression models with zero intercepts (method 1) are always biased and underestimate the asymmetry, and they should not be used. While method 2 removes means separately for the positive and negative values of the independent and corresponding dependent variables, method 1 removes means from independent and dependent variables for the entire data set. In the ocean-atmosphere coupling framework, method 1 thus implicitly assumes that a neutral ocean leads to no atmospheric anomaly, which does not hold if there is asymmetry. The single degree of freedom lost in setting the intercept in method 2 is well made up by avoiding the biased slope estimates of method 2. Composites are also biased and underestimate the asymmetry, strongly for small thresholds but less so for very large thresholds (which may be unattainable with observations). However, the errors are then quite large if the sample is limited.

To illustrate the differences between the three methods investigated here using observations, we have estimated the asymmetry of the tropical Pacific SST anomaly associated with positive and negative values of the Niño3.4 index in DJF in the period 1948–2018, as done in many studies. All three methods nicely show the westward shift of maximum SST amplitude in La Niña events and the substantial amplitude along the South American coast in El Niño events. While the differences between methods are rather small, the local SST amplitudes consistently show the largest asymmetry for regression method 2. The associated SLP anomalies show a strong asymmetry in all cases, with a strong Aleutian Low strengthening during El Niño events and a much smaller, southwestward shifted low during La Niña events. Consistent with our mathematical derivation and synthetic example, the Aleutian Low response to El Niño is strongest for regression method 2 and weakest for regression method 1,

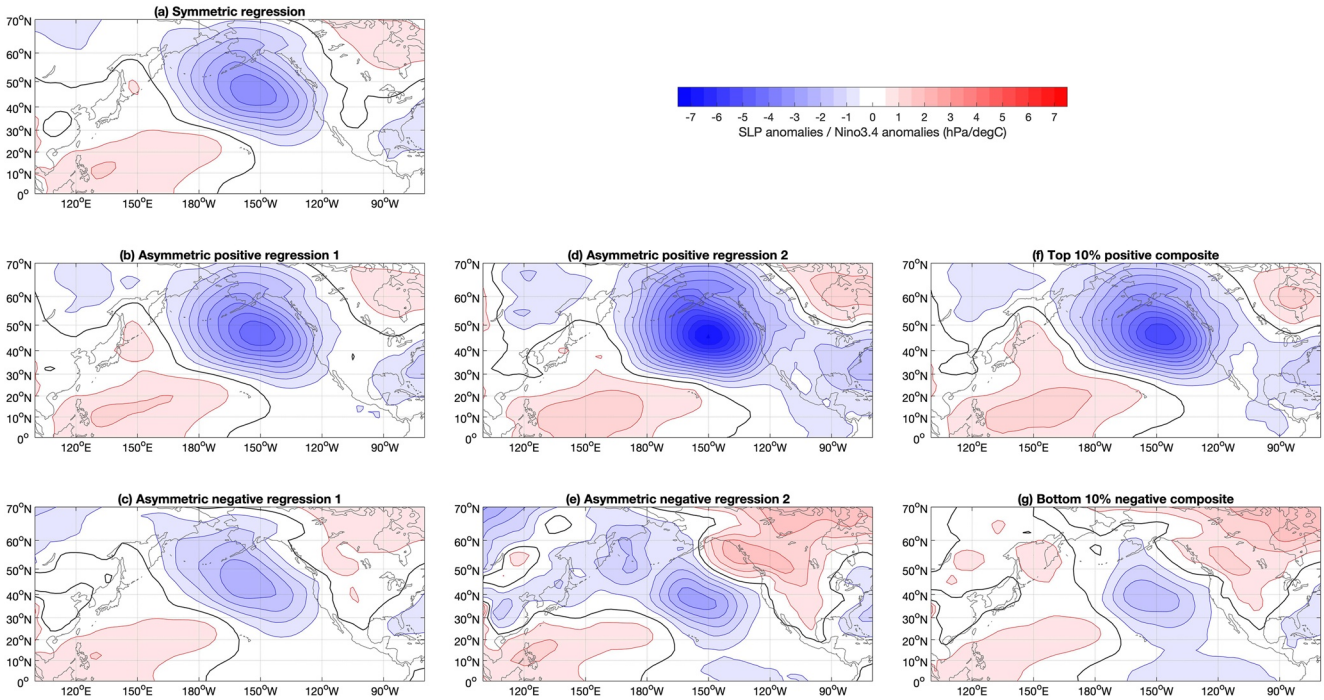

Figure 4. Sea level pressure in JFM (in hPa/°C, contour interval 0.5 hPa/°C) associated with positive and negative values of the Niño3.4 index in DJF. Estimates were made by (a) standard regression, (b and c) asymmetric regression 1, (d and e) asymmetric regression 2, and (f and g) composites based on a 10% threshold (seven El Niño and seven La Niña events).

while compositing based on a high 10% threshold provide intermediate results. The latter are consistent with the composites in Mezzina et al. (2022). Although the true asymmetry is not known in the observational data, the results confirm that compositing tend to underestimate asymmetry and suggest that asymmetric regression with non-zero intercepts (unbiased method 2) should be preferred. For data that can be highly skewed, however, such as precipitation signals, the linear assumption in asymmetric regression is limiting, and a probabilistic approach for detecting asymmetric ENSO teleconnections may be preferable, such as using contingency tables (e.g., Lenssen et al., 2020; Mason & Goddard 2012).

In recent studies of the atmospheric response to SST or other oceanic anomalies, multiple regressions have been increasingly used to distinguish their impacts from the influence of concomitant factors such as sea-ice concentration, or snow cover (e.g., Liu et al., 2008; Révelard et al., 2018; Simon et al., 2020). Asymmetry in the responses could not be estimated by applying method 2 to multiple linear regression, since the positive and negative values of each predictor would not occur simultaneously, thus preventing an appropriate definition of demeaned variables Y_p and Y_n. If asymmetry is only expected in the response to one predictor, method 2 could be applied to its positive and negative values, while including in each case the additional concomitant predictors, but two different slopes and significance might be obtained for these other predictors, despite the implicit assumption of symmetry. However, if only weak correlation between positive and negative values of multiple predictors is expected, as could be the case if the predictors are (orthogonal) principal components of the same variable (e.g., tropical SST anomalies), sequential estimation with method 2 may provide acceptable results. Using method 1 and separating each predictor time series into positive and negative sequences is feasible and was used by Frankignoul et al. (2011) and Révelard et al. (2016) to asymmetrically remove ENSO teleconnections based on two ENSO indices, but such estimates are biased, as shown here. In addition, if there are many regressors, the increased dimensionality might result in overfitting or collinearity, although series of positive and negative phases would be pairwise uncorrelated. Hence, the generalization to multiple asymmetric regression requires further investigation.

Data Availability Statement

The SST data were downloaded from https://www.metoffice.gov.uk/hadobs/hadisst and the SLP data from https://psl.noaa.gov/data/gridded/data.ncep.reanalysis.html. The Matlab code used in the synthetic example is available from the authors on request.

Acknowledgments
This research was supported by NSF's Grant AGS-2040073. Comments by the reviewers and Arnaud Czaja are thankfully acknowledged.

References

Deser, C., Simpson, I. R., McKinnon, K. A., & Phillips, A. S. (2017). The Northern Hemisphere extratropical atmospheric circulation response to ENSO: How well do we know it and how do we evaluate models accordingly. *Journal of Climate*, *30*(13), 5059–5082. https://doi.org/10.1175/JCLI-D-16-0844.1

Frankignoul, C., Sennéchael, N., Kwon, Y.-O., & Alexander, M. A. (2011). Influence of the meridional shifts of the Kuroshio and the Oyashio Extensions on the atmospheric circulation. *Journal of Climate*, *24*(3), 762–777. https://doi.org/10.1175/2010jcli3731.1

Hardiman, S. C., Dunstone, N. J., Scaife, A. A., Smith, D. M., Ineson, S., Lim, J., & Fereday, D. (2019). The impact of strong El Niño and La Niña events on the North Atlantic. *Geophysical Research Letters*, *46*(5), 2974–2883. https://doi.org/10.1029/2018gl081776

Kistler, R., Kalnay, E., Collins, W., Saha, S., White, G., Woollen, J., et al. (2001). The NCEP-NCAR 50-year reanalysis: Monthly means CD-ROM and documentation. *Bulletin America Meteorology Social*, *82*(2), 247–267. https://doi.org/10.1175/1520-0477(2001)082<0247:tnnyrm>2.3.co;2

Lenssen, N. J. L., Goddard, L., & Mason, S. (2020). Seasonal forecast skill of ENSO teleconnection maps. *Weather and Forecasting*, *35*(6), 2387–2406. https://doi.org/10.1175/WAF-D-19-0235.1

Liu, Z., Wen, N., & Liu, Y. (2008). On the assessment of nonlocal climate feedback. Part I: The generalized equilibrium feedback analysis. *Journal of Climate*, *21*(1), 134–148. https://doi.org/10.1175/2007jcli1826.1

Mason, S. J., & Goddard, L. (2001). Probabilistic precipitation anomalies associated with ENSO. *Bulletin of the American Meteorological Society*, *82*, 619–638. https://doi.org/10.1175/1520-0477(2001)082<0619:PPAAWE>2.3.CO;2

Mezzina, B., García-Serrano, J., Bladé, I., Palmeiro, F. M., Batté, L., Ardilouze, C., et al. (2022). Multi-model assessment of the late-winter extra-tropical response to El Niño and La Niña. *Climate Dynamics*, *58*(7–8), 1995–1986. https://doi.org/10.1007/s00382-020-05415-y

Okumura, Y. M., & Deser, C. (2010). Asymmetry in the duration of El Niño and La Niña. *Journal of Climate*, *23*(21), 5826–5843. https://doi.org/10.1175/2010jcli3592.1

Rayner, N. A., Parker, D. E., Horton, E. B., Folland, C. K., Alexander, L. V., Rowell, D. P., et al. (2003). Global analyses of sea surface temperature, sea ice, and night marine air temperature since the late nineteenth century. *Journal of Geophysical Research: Atmosphere*, *108*(D14), 4407. https://doi.org/10.1029/2002jd002670

Révelard, A., Frankignoul, C., & Kwon, Y.-O. (2018). A multivariate estimate of the cold season atmospheric response to North Pacific SST variability. *Journal of Climate*, *31*(7), 2771–2796. https://doi.org/10.1175/jcli-d-17-0061.1

Révelard, A., Frankignoul, C., Sennéchael, N., Kwon, Y.-O., & Qiu, B. (2016). Influence of the decadal variability of the Kuroshio Extension on the atmospheric circulation in the cold season. *Journal of Climate*, *29*(6), 2123–2144. https://doi.org/10.1175/jcli-d-15-0511.1

Seo, H., Kwon, Y.-O., Joyce, T. M., & Ummenhofer, C. C. (2017). Predominant nonlinear forced response of the extratropical atmosphere to meridional shifts in the Gulf Stream. *Journal of Climate*, *30*(23), 9679–9702. https://doi.org/10.1175/JCLI-D-16-0707.1

Seo, H., Kwon, Y.-O., & Park, J.-J. (2014). On the effect of marginal sea SST variability on the North Pacific atmospheric circulation. *Journal of Geophysical Research: Atmospheres*, *119*(2), 418–444. https://doi.org/10.1002/2013JD020523

Simon, A., Frankignoul, C., Gastineau, G., & Kwon, Y.-O. (2020). An observational estimate of the direct response of the cold season atmospheric circulation to the Arctic Sea Ice Loss. *Journal of Climate*, *33*(9), 3863–3882. https://doi.org/10.1175/JCLI-D-19-0687.1

Smirnov, D., Newman, M., Alexander, M. A., Kwon, Y.-O., & Frankignoul, C. (2015). Investigating the local atmospheric response to a realistic shift in the Oyashio sea surface temperature front. *Journal of Climate*, *28*(3), 1126–1147. https://doi.org/10.1175/jcli-d-14-00285.1

Timmermann, A., An, S. I., Kug, J. S., Jin, F. F., Cai, W., Capotondi, A., et al. (2018). El-Niño-Southern Oscillation complexity. *Nature*, *559*(7715), 535–545. https://doi.org/10.1038/s41586-018-0252-6